



Article

The Anti-Senescence Activity of Cytokinin Arabinosides in Wheat and Arabidopsis Is Negatively Correlated with Ethylene Production

Zuzana Kučerová ¹ , Marek Rác ¹, Jaromír Mikulík ², Ondřej Plíhal ², Pavel Pospíšil ¹,
Magdaléna Bryksová ³ , Michaela Sedlářová ⁴ , Karel Doležal ^{2,3} and Martina Špundová ^{1,*}

¹ Department of Biophysics, Centre of the Region Haná for Biotechnological and Agricultural Research, Faculty of Science, Palacký University, Šlechtitelů 27, CZ-78371 Olomouc, Czech Republic; zuzana.kucerova@upol.cz (Z.K.); marek.rac@upol.cz (M.R.); pavel.pospisil@upol.cz (P.P.)

² Laboratory of Growth Regulators, Faculty of Science, Palacký University and Institute of Experimental Botany AS CR, Šlechtitelů 27, CZ-78371 Olomouc, Czech Republic; jaromir.mikulik@upol.cz (J.M.); ondrej.plihal@upol.cz (O.P.); karel.dolezal@upol.cz (K.D.)

³ Department of Chemical Biology and Genetics, Centre of the Region Haná for Biotechnological and Agricultural Research, Faculty of Science, Palacký University, Šlechtitelů 27, CZ-78371 Olomouc, Czech Republic; magdalena.bryksova@upol.cz

⁴ Department of Botany, Faculty of Science, Palacký University, Šlechtitelů 27, CZ-78371 Olomouc, Czech Republic; michaela.sedlarova@upol.cz

* Correspondence: martina.spundova@upol.cz; Tel.: +420-585-634-512

Received: 15 October 2020; Accepted: 28 October 2020; Published: 30 October 2020



Abstract: Leaf senescence, accompanied by chlorophyll breakdown, chloroplast degradation and inhibition of photosynthesis, can be suppressed by an exogenous application of cytokinins. Two aromatic cytokinin arabinosides (6-benzylamino-9- β -D-arabinofuranosylpurines; BAPAs), 3-hydroxy- (3OHBAPA) and 3-methoxy- (3MeOBAPA) derivatives, have recently been found to possess high anti-senescence activity. Interestingly, their effect on the maintenance of chlorophyll content and maximal quantum yield of photosystem II (PSII) in detached dark-adapted leaves differed quantitatively in wheat (*Triticum aestivum* L. cv. Aranka) and Arabidopsis (*Arabidopsis thaliana* L. (Col-0)). In this work, we have found that the anti-senescence effects of 3OHBAPA and 3MeOBAPA in wheat and Arabidopsis also differ in other parameters, including the maintenance of carotenoid content and chloroplasts, rate of reduction of primary electron acceptor of PSII (Q_A) as well as electron transport behind Q_A , and partitioning of absorbed light energy in light-adapted leaves. In wheat, 3OHBAPA had a higher protective effect than 3MeOBAPA, whereas in Arabidopsis, 3MeOBAPA was the more efficient derivative. We have found that the different anti-senescent activity of 3OHBAPA and 3MeOBAPA was coupled to different ethylene production in the treated leaves: the lower the ethylene production, the higher the anti-senescence activity. 3OHBAPA and 3MeOBAPA also efficiently protected the senescing leaves of wheat and Arabidopsis against oxidative damage induced by both H₂O₂ and high-light treatment, which could also be connected with the low level of ethylene production.

Keywords: cytokinin derivative; ethylene; senescence; chlorophyll fluorescence; wheat; Arabidopsis; phytohormone; oxidative stress; photosystem II

1. Introduction

Phytohormones cytokinins (CKs) have a crucial role in almost all stages of plant growth and development, including senescence. Senescence is a highly organized and controlled process that is characterized by dramatic structural and functional changes, such as degradation of photosynthetic

pigments and inhibition of photosynthesis (e.g., [1–3]), and by extensive changes in gene expression [4]. An exogenous application of CKs typically delays senescence-induced decreases in chlorophyll (Chl) and carotenoid content, inhibition of photosynthesis, degradation of proteins, pigment–protein complexes and whole chloroplasts, as well as membrane deterioration (e.g., [3,5–9]). The anti-senescence activity of CKs is related to the downregulation of senescence-associated genes (SAGs) [10] and upregulation of genes encoding components of photosynthetic light-harvesting complexes [11].

From an agricultural point of view, leaf senescence is one of the major traits that negatively affects crop production, and therefore the delay of this process represents an ideal target for improving crop yield and quality [12]. One of the natural CKs that is used both in agriculture [13] and biotechnology is the aromatic CK 6-benzylaminopurine (BAP), mainly because of its activity, affordability, and stability in plants [14,15]. BAP has significant anti-senescence activity and its exogenous application effectively delays senescence-induced changes (e.g., [3,8,9]). However, under certain conditions, BAP can have negative effects on primary root development, lateral root branching, or shoot formation in vitro (e.g., [16–19]). When applied at higher concentrations or in combination with light, BAP can even accelerate senescence [11,20,21]. These findings led to the search for aromatic CK derivatives that would not exhibit these negative effects on plant growth and development [22]. Several previously prepared compounds have been shown to be more efficient in delaying senescence than unmodified BAP, including those with hydroxy- or methoxy-groups introduced to the benzyl ring (e.g., [5,23,24]).

In our previous work, novel 6-benzylamino-9- β -D-arabinofuranosylpurines (BAPAs) were synthesized [25] and their unique mode of action has been described [26]. BAPAs have high anti-senescence activity, but they have generally low interactions with the CK pathway and thus also very low activity in other CK-regulated processes and no negative effects on root/shoot development [26]. We have observed that the application of BAPAs induced a massive transcriptional reprogramming from photosynthesis toward defense responses, including the elicitation of several MAPK modules, suggesting an induction of a pathogen-associated molecular patterns (PAMP)-like response [26]. This response was accompanied by delaying senescence. A comparison of the anti-senescence activity of two selected BAPAs, 3-hydroxy- (3OHBAPA) and 3-methoxy- (3MeOBAPA) derivatives (see Figure 1), indicated that their protective effect during senescence (maintenance of Chl content and maximal quantum yield of photosystem II (PSII)) differs quantitatively in wheat and Arabidopsis: 3OHBAPA had higher protective effect in wheat, while in Arabidopsis 3MeOBAPA was more efficient.

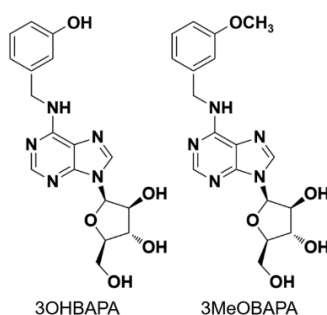


Figure 1. Structure of 6-(3-hydroxybenzylamino)-9- β -D-arabinofuranosylpurine (3OHBAPA, left) and 6-(3-methoxybenzylamino)-9- β -D-arabinofuranosylpurine (3MeOBAPA, right).

Here, we have investigated whether the different effects of 3OHBAPA and 3MeOBAPA on the senescence of detached wheat (*Triticum aestivum* L. cv. Aranka) and *Arabidopsis thaliana* L. (Col-0) leaves will also manifest in the maintenance of other parameters related to photosynthetic apparatus and its function. We have evaluated the changes in carotenoid content and chloroplasts, rate of reduction of primary electron acceptor of PSII (Q_A) and electron transport behind Q_A , and changes in the partitioning of absorbed light energy in light-adapted leaves. We have also explored the possibility that the different anti-senescent activity of 3OHBAPA and 3MeOBAPA in both plant models is related

to a different level of ethylene production in the treated leaves, as ethylene is known to co-determine the progression of senescence in plant samples treated by anti-senescence compounds [27]. Finally, we have evaluated whether 3OHBAPA and 3MeOBAPA can protect senescing leaves of wheat and Arabidopsis against oxidative damage induced by both H₂O₂ and high-light treatment.

2. Results and Discussion

2.1. Senescence-Induced Changes in Detached Leaves of Wheat and Arabidopsis

The decrease in photosynthetic pigment content, deterioration of chloroplasts, and the loss of photosynthetic activity are typical phenomena of leaf senescence [1–3,7]. In our case, after six days of dark-induced senescence of detached wheat and Arabidopsis leaves, the content of Chl decreased significantly (Figure 2A). In line with our previous results [26], the decline in Chl content was more pronounced in the case of Arabidopsis leaves, which reflected a higher progression of senescence compared to wheat (Figure 2A). A similar trend was observed in the decrease in carotenoid content (Figure 2C). The relative rate of degradation of Chl *a* and Chl *b* differed between the leaves of wheat and Arabidopsis, as evidenced by different changes in the Chl *a/b* ratio (Figure 2B). The decrease in the ratio found in wheat indicated a higher degradation of Chl *a*, while in the Arabidopsis leaves Chl *b* degraded faster, which resulted in a higher Chl *a/b* ratio (Figure 2B).

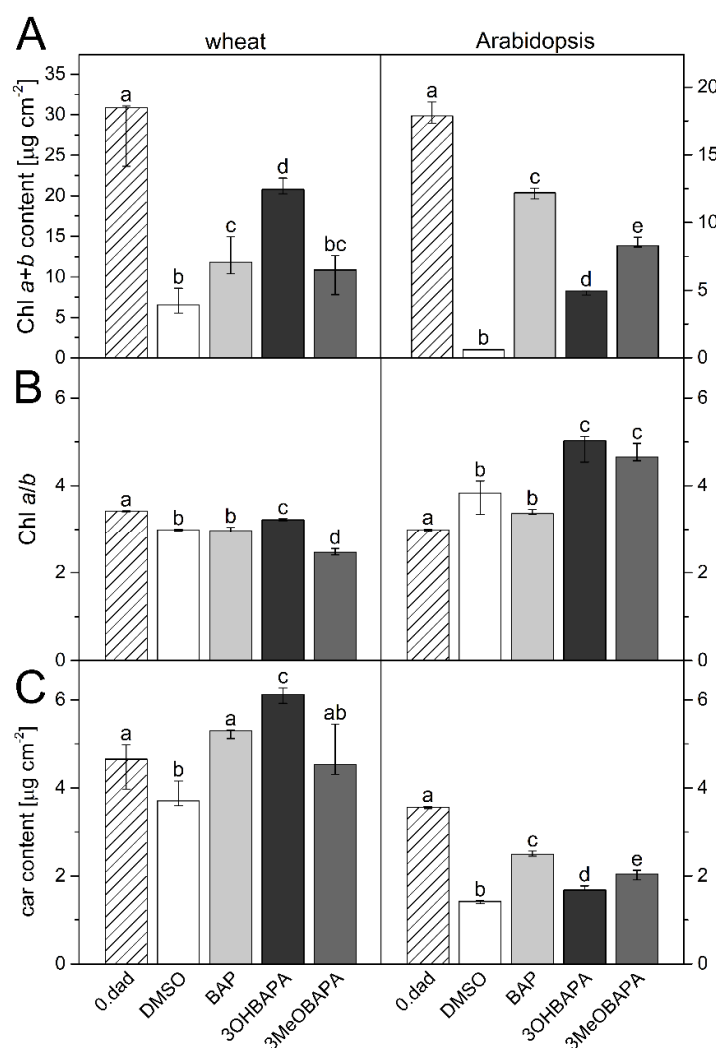


Figure 2. (A) Chlorophyll (Chl) *a+b* content; (B) Chl *a/b* ratio and (C) carotenoid (car) content in control (0. dad) and detached leaves of wheat and Arabidopsis after 6 days of dark incubation in 0.1% DMSO

or $10\text{-}\mu\text{mol}\cdot\text{L}^{-1}$ solutions of 6-benzylaminopurine (BAP), 3OHBAPA and 3MeOBAPA. Medians and quartiles are shown ($n = 5$). Different letters indicate a statistically significant difference between treatments within a plant species ($p < 0.05$; Student's unpaired t -test).

Since the progressive decline in photosynthetic pigment contents suggests chloroplast degradation, confocal microscopy was performed to compare the chloroplast integrity in freshly detached leaves ("0. dad") and in the leaves senescing for six days in the dark ("DMSO"; Figure 3). In senescing wheat leaves, the chloroplasts were still partially preserved, although their deterioration and aggregation was apparent (Figure 3A). In Arabidopsis, chloroplast autofluorescence was no longer detectable (Figure 3B), suggesting chloroplast degradation, which implies, together with apparent impairment of tissue structure, more advanced senescence compared to wheat.

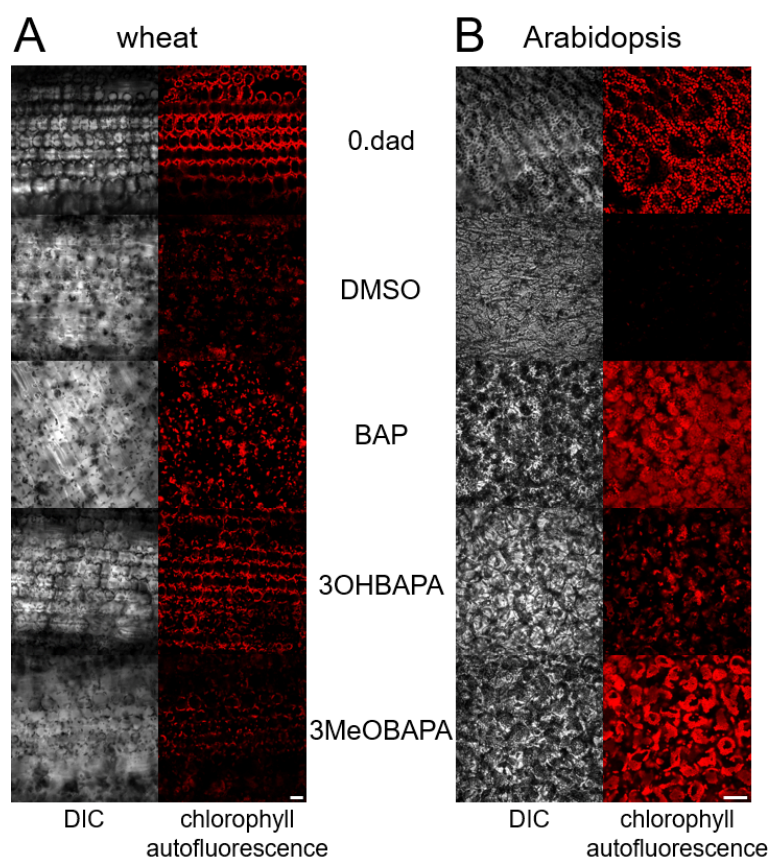


Figure 3. Confocal micrographs of freshly detached (0. dad) (A) wheat and (B) Arabidopsis leaves and leaves incubated in 0.1% DMSO or $10\text{-}\mu\text{mol}\cdot\text{L}^{-1}$ solutions of BAP, 3MeOBAPA and 3OHBAPA in the dark for 6 days. Scale bars represent $50\ \mu\text{m}$. DIC, differential interference contrast.

The different extent of senescence in wheat and Arabidopsis was also manifested at the level of PSII function, whose maintenance was estimated from the measurement of Chl fluorescence parameters (Figure 4). We measured Chl fluorescence induction transient (OJIP curve) to monitor the rate of excitation supply to reaction center (RCII), reduction of primary electron acceptor of PSII (Q_A), and subsequent electron transport behind Q_A [28] during the first (milli)seconds of illumination of dark-adapted leaves. In wheat leaves, both $(dV/dt)_0$ and V_j parameters increased (Figure 4A,B), indicating the acceleration of excitation supply to RCII and Q_A reduction and inhibition of electron transport behind Q_A . Unlike in wheat, a decrease in $(dV/dt)_0$ was found in Arabidopsis leaves, while V_j increased to its maximal value ($=1$). These changes indicate a strong impairment of PSII, involving minimal delivery of excitations to RCII as well as extreme inhibition of electron transfer from Q_A^- . In the senescent Arabidopsis leaves, the inhibition of the excitation supply to RCII could

be partially related to the increased Chl *a/b* ratio (Figure 2B), which reflects higher degradation of light-harvesting complexes of PSII (LHCII) compared to RCII [29].

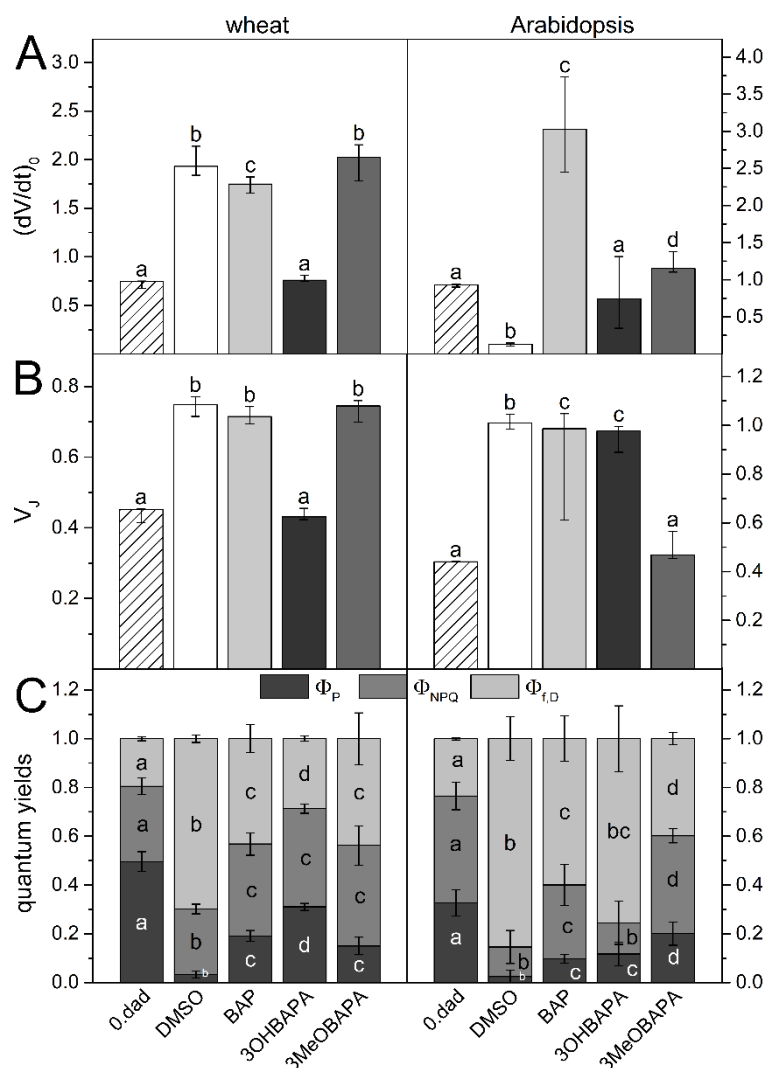


Figure 4. (A) The initial slope of the O–J Chl fluorescence rise $(dV/dt)_0$, (B) the relative variable fluorescence at the J step (V_j) and (C) quantum yields of photosystem II (PSII) photochemistry (Φ_P), regulatory non-photochemical quenching (Φ_{NPQ}) and non-regulatory dissipation processes ($\Phi_{f,D}$) in control (0. dad) and detached leaves of wheat and Arabidopsis after 6 days of dark-incubation in 0.1% DMSO or $10\text{-}\mu\text{mol}\cdot\text{L}^{-1}$ solutions of BAP, 3OHBAPA and 3MeOBAPA. Medians and quartiles are presented ($n = 5\text{--}12$). Different letters indicate a statistically significant difference between treatments within a plant species ($p < 0.05$; Student's unpaired *t*-test).

Further information on senescence-induced changes in the PSII function was obtained by measurement of quantum yields Φ_P , Φ_{NPQ} and $\Phi_{f,D}$. These parameters, measured during exposition of leaves to actinic light, reflect the partitioning of absorbed light energy for PSII photochemistry (Φ_P) and for regulated (Φ_{NPQ}) and non-regulated ($\Phi_{f,D}$) non-photochemical processes [30]. Steady-state values of Φ_P , Φ_{NPQ} , and $\Phi_{f,D}$ measured after a 7-min exposition of the senescent leaves to actinic light are presented (Figure 4C). A higher decrease in Φ_P and Φ_{NPQ} , and a more pronounced increase in $\Phi_{f,D}$ was found in Arabidopsis compared to wheat (Figure 4C). These results again indicate very strong impairment of PSII function in senescent Arabidopsis leaves connected with the low ability of photosynthetic apparatus to regulate dissipation of excess light energy, which subsequently can result in oxidative damage [31].

2.2. Comparison of the Anti-Senescence Activity of BAP and CK Arabinosides in Wheat and Arabidopsis Leaves

It is well known that the senescence-induced changes can be effectively delayed by the exogenous application of CKs. The aromatic cytokinin BAP is known to be stable in plants and highly active in delaying senescence (e.g., [3,5,8,9]). In line with the previously published results, the exogenous application of BAP slowed down the senescence-induced decrease in Chl and carotenoid content and partially suppressed deterioration of chloroplasts in both wheat and Arabidopsis (Figures 2 and 3). However, the effect of BAP on parameters reflecting PSII function during the initial phase of transition of photosynthetic apparatus from a dark- to light-adapted state (the OJIP transient) was not so convincing. The only distinct effect of BAP was found for $(dV/dt)_0$ in Arabidopsis. Unlike in the mock-treated leaves ("DMSO"), in the BAP-treated leaves the parameter $(dV/dt)_0$ increased pronouncedly, indicating faster excitation delivery, probably due to the suppression of the preferential degradation of LHClI observed in the mock-treated Arabidopsis leaves. A minimal protective effect of BAP on excitation delivery to RCII, reduction in Q_A and electron transport behind Q_A was found in the wheat leaves (Figure 4A,B). A similar effect of BAP has already been reported by Špundová [32] in wheat, but only 7 days after leaf detachment. In leaves senescing for 4 days, BAP significantly protected electron transfer behind Q_A , as indicated by the non-increased V_J . Since a pronounced protective effect of BAP on excitation delivery to RCII ($dV/dt)_0$ and electron transport behind Q_A (V_J) was also found by Janečková [3] in detached leaves of barley senescing for 4 days, it seems that BAP protects these photosynthetic reactions especially at earlier stages of senescence and later its effect weakens.

The senescence-induced changes in the partitioning of absorbed light energy were partially reduced in the BAP-treated leaves. The PSII photochemistry and regulatory non-photochemical quenching were more effective and the increase in the yield of non-regulated energy dissipation was lower compared to the mock-treated leaves (Figure 4C). This protective effect of BAP on PSII photochemistry corresponds with the maintenance of the maximal quantum yield of PSII photochemistry (F_V/F_M) found in our previous work [26].

Based on the estimation of overall Chl content in detached leaves of wheat and Arabidopsis, we have recently found that CK arabinosides have similar or even higher anti-senescence activity than BAP [25,26]. Two of them, 3OHBAPA and 3MeOBAPA derivatives, have been found to have a strong positive effect on F_V/F_M (measured in the dark-adapted state of the senescent leaves) [26]. Interestingly, this effect differed quantitatively in wheat and Arabidopsis. 3OHBAPA had a higher protective effect in wheat, while 3MeOBAPA was more effective in Arabidopsis. In both plant species, the CK arabinosides were more effective in the maintenance of PSII function than BAP [26].

In this work, we have compared the effect of 3OHBAPA, 3MeOBAPA and BAP on senescence-induced changes in other parameters that characterize the status of photosynthetic apparatus. Among the treated senescing leaves, relative differences in carotenoid contents corresponded to those of Chl (compare Figure 2A,C). In wheat, the carotenoid content was maintained similarly in BAP- and 3MeOBAPA-treated leaves, whereas in leaves treated with 3OHBAPA many more carotenoids (even more than in the freshly detached leaves) were found, confirming the more positive effect of this CK arabinoside. In Arabidopsis, the efficiency of 3MeOBAPA was lower in comparison with BAP, but higher when compared to 3OHBAPA (Figure 2C). Similar trends were found at the level of chloroplast integrity, evaluated by confocal microscopy (Figure 3). In the case of wheat, senescence-induced deterioration of chloroplasts was similar in the BAP- and 3MeOBAPA-treated leaves, whereas in the leaves treated by 3OHBAPA chloroplasts were better preserved (Figure 3A). On the contrary, in Arabidopsis, the protective effect of 3OHBAPA was the weakest (Figure 3B).

The senescence-induced impairment of PSII function was suppressed almost completely by 3OHBAPA in wheat and 3MeOBAPA in Arabidopsis. The excitation supply to RCII, Q_A reduction and electron transport behind Q_A were highly maintained, as indicated by the unchanged values of $(dV/dt)_0$ and V_J compared to non-senescent leaves (Figure 4A,B). Interestingly, in the 3MeOBAPA-treated leaves of Arabidopsis, the excitation supply into RCII was not accelerated (as in the BAP-treated leaves, Figure 4A), which corresponds to a higher degradation of LHClI compared to RCII, indicated also

by the increased Chl *a/b* ratio (Figure 2B). This result is in line with the RNA-seq gene expression analysis in our previous study, where we have shown that the genes encoding LHCII components were downregulated in 3MeOBAPA-treated leaves [26]. The absence of increased delivery of excitations to RCII could contribute to the protection of photosynthetic apparatus from excess excitations and to the maintenance of the partitioning of absorbed light energy documented by minimal changes of Φ_P , Φ_{NPQ} and $\Phi_{f,D}$ (Figure 4C). Interestingly, CK ribosides synthesized by Vylíčilová [11] caused the upregulation of LHCII genes and an increase in the relative abundance of LHCII [11], implying a different mechanism of action of CK arabinosides and CK ribosides.

In summary, 3OHBAPA had the highest anti-senescence activity in wheat, followed by 3MeOBAPA and BAP, whose activity was similar. In Arabidopsis, 3MeOBAPA was less efficient than BAP in the maintenance of photosynthetic pigment content, but it was more efficient in the maintenance of PSII function. At the same time, when compared to 3OHBAPA, 3MeOBAPA had higher anti-senescence activity, as documented by the changes in all studied parameters.

It has been shown that different activity of anti-senescence compounds can be associated with their influence on ethylene production in the detached dark-incubated leaves [27]. It is known that the exogenous application of CKs stimulates the production of ethylene [33,34]. As opposed to the positive effect of CKs on plant and leaf longevity, ethylene is known for being the accelerator of senescence [35]. Thus, the rate of the stimulation of ethylene production by exogenously applied CK can co-determine a resultant senescence-delaying effect—i.e., the anti-senescence activity of CK.

We have evaluated the effect of the compounds on ethylene production in wheat and Arabidopsis leaves. As expected, the ethylene production in BAP-treated leaves was higher compared to the mock-treated leaves (Figure 5). Interestingly, no stimulation of ethylene production was observed in the wheat leaves treated by 3OHBAPA and in Arabidopsis leaves treated by 3MeOBAPA. A moderately stimulated ethylene production was observed in the 3MeOBAPA-treated wheat leaves and 3OHBAPA-treated leaves of Arabidopsis (Figure 5). Thus, the differences in the rate of ethylene production corresponded generally to the quantitative differences of anti-senescence activity between BAP and BAPAs, as well as between 3OHBAPA and 3MeOBAPA: the lower the ethylene production, the higher the anti-senescence activity.

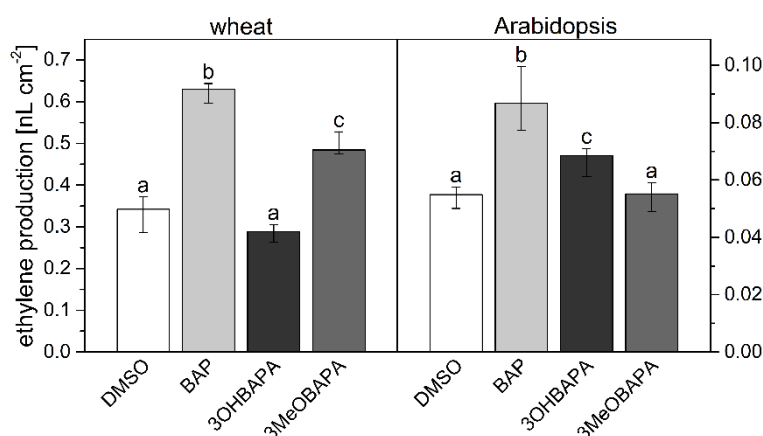


Figure 5. Ethylene production in detached leaves of wheat and Arabidopsis incubated in 0.1% DMSO or 10- $\mu\text{mol}\cdot\text{L}^{-1}$ solutions of BAP, 3OHBAPA and 3MeOBAPA and kept sealed in 8-mL vials in darkness for 6 days. Medians and quartiles are presented ($n = 5-9$). Different letters indicate a statistically significant difference between treatments within a plant species ($p < 0.05$; Student's unpaired *t*-test).

2.3. Species-Specific Effects of BAPAs Treatment in the Protection Against Induced Oxidative Damage

It has been shown that the inhibition of ethylene production not only suppresses leaf senescence, but it also enhances the tolerance of plants to abiotic stresses, including H_2O_2 - and high light (HL)-induced oxidative stress [36]. As no stimulation of ethylene production was found in wheat leaves

treated by 3OHBAPA and Arabidopsis leaves treated by 3MeOBAPA (Figure 5), we hypothesized that the mentioned BAPA treatments could provide a more efficient protection of leaves against oxidative damage induced by H₂O₂- and HL-treatment than the BAP treatment.

For a comparison of the protective effect of CK arabinosides and BAP, senescent leaves were exposed to exogenous H₂O₂ (5 mmol·L⁻¹) and the level of oxidative damage was evaluated using ultra-weak photon emission (UPE) [37]. In the mock-treated leaves, the H₂O₂ treatment caused pronounced oxidative damage as indicated by the high UPE ratio (Figure 6). In wheat, the protective effect indicated by the lower UPE ratio was observed only in leaves treated with 3OHBAPA. In Arabidopsis, both BAP and 3MeOBAPA reduced the oxidative damage, 3MeOBAPA being more effective (Figure 6).

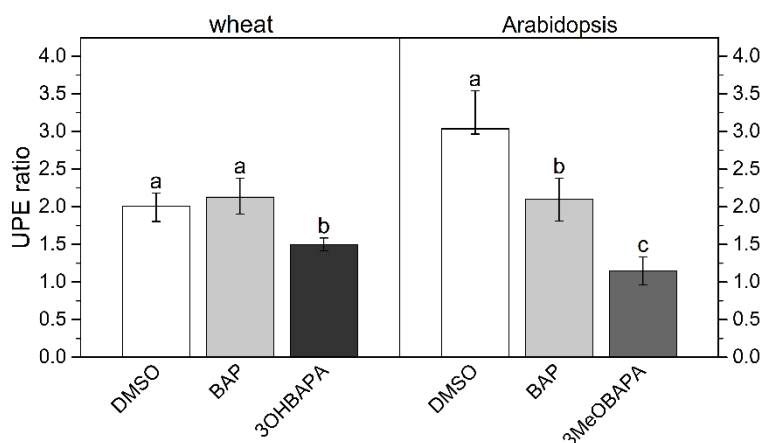


Figure 6. Ratio of ultra-weak photon emission (UPE) intensity after/before application of H₂O₂ in detached leaves of wheat and Arabidopsis dark-incubated for 6 days in 0.1% DMSO or 10- μ mol·L⁻¹ solutions of BAP, 3OHBAPA or 3MeOBAPA. Medians and quartiles are presented ($n = 4$). Different letters indicate a statistically significant difference between treatments within a plant species ($p < 0.05$; Student's unpaired t -test).

In the following experiment, we exposed the senescent leaves to HL (500 μ mol photons·m⁻²·s⁻¹) and estimated cell membrane damage using the measurement of ion leakage by conductivity, accumulation of lipid hydroperoxides (LOOHs; as primary products of lipid peroxidation and markers of oxidative damage) by confocal microscopy, and maintenance of the maximal quantum yield of PSII photochemistry (F_V/F_M), which reflects the extent of photoinhibition or photodamage of PSII. The exposure of senescing leaves to HL led to a strong oxidative damage, as indicated by progressive deterioration of cell membranes during 8 h of HL treatment (Figure 7), and by LOOH accumulation (Figure 8) and photoinhibition of PSII (Figure 9) after 4 h of HL treatment. The oxidative damage was suppressed by the exogenous application of BAP, although its protective effect was quite low. The HL-induced membrane deterioration and PSII photoinhibition were attenuated in the BAP-treated leaves of both wheat and Arabidopsis; LOOH accumulation was reduced only in Arabidopsis (Figures 7–9).

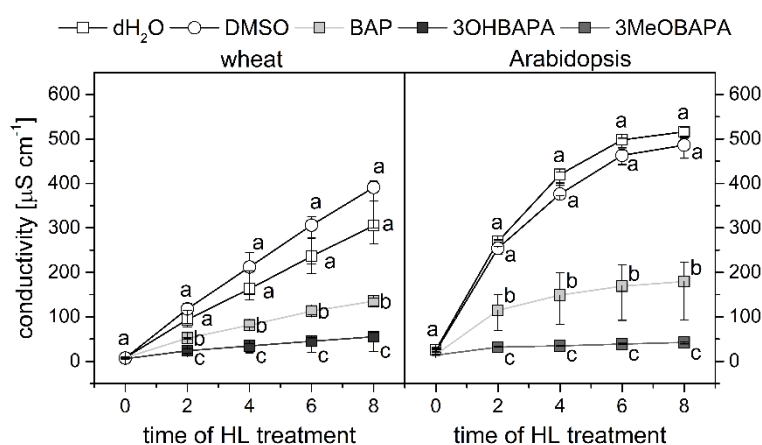


Figure 7. Conductivity as a measure of cell membrane damage in wheat- and Arabidopsis-detached leaves incubated in deionized water (dH₂O), 0.1% DMSO, 10- $\mu\text{mol}\cdot\text{L}^{-1}$ solutions of BAP, 3OHBAPA or 3MeOBAPA. Before high-light treatment (HL; 500 $\mu\text{mol photons}\cdot\text{m}^{-2}\cdot\text{s}^{-1}$) for up to 8 h leaves were incubated in the dark for 6 days. Medians and quartiles are presented ($n = 7$). Different letters indicate a statistically significant difference between treatments within a plant species and particular time point ($p < 0.05$; Student's unpaired t -test).

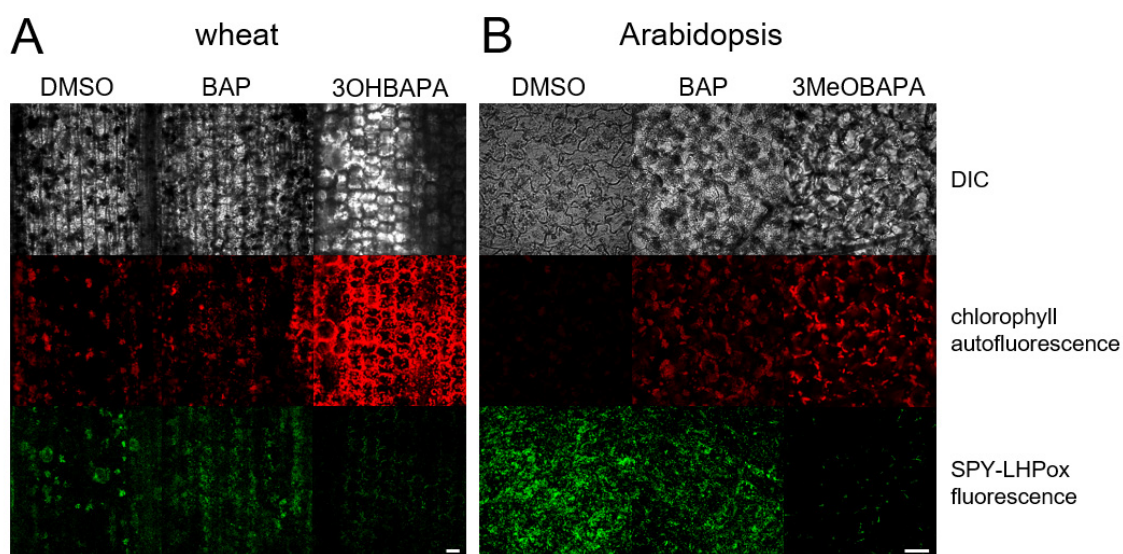


Figure 8. In vivo imaging of lipid hydroperoxides (LOOHs) using fluorescent probe SPY-LHP in (A) wheat and (B) Arabidopsis leaves kept in the dark for 6 days and subsequently exposed to high light (500 $\mu\text{mol photons}\cdot\text{m}^{-2}\cdot\text{s}^{-1}$) for 4 h. Detached leaves were incubated in 0.1% DMSO or 10- $\mu\text{mol}\cdot\text{L}^{-1}$ solutions of BAP, 3OHBAPA or 3MeOBAPA. Scale bars represent 50 μm . DIC, differential interference contrast.

As expected, 3OHBAPA in wheat and 3MeOBAPA in Arabidopsis were more effective in the protection of senescing leaves from oxidative damage than BAP. BAPs markedly reduced the HL-induced cell membrane damage (Figure 7), accumulation of LOOHs (Figure 8), as well as PSII photoinhibition (Figure 9). We suppose that in the case of HL-treated wheat leaves, the high protective effect of 3OHBAPA can be mainly ascribed to the completely maintained xanthophyll cycle (Figure 9C) together with the high content of xanthophylls (Figure 10), both of which are known to be important for photoprotection [38,39].

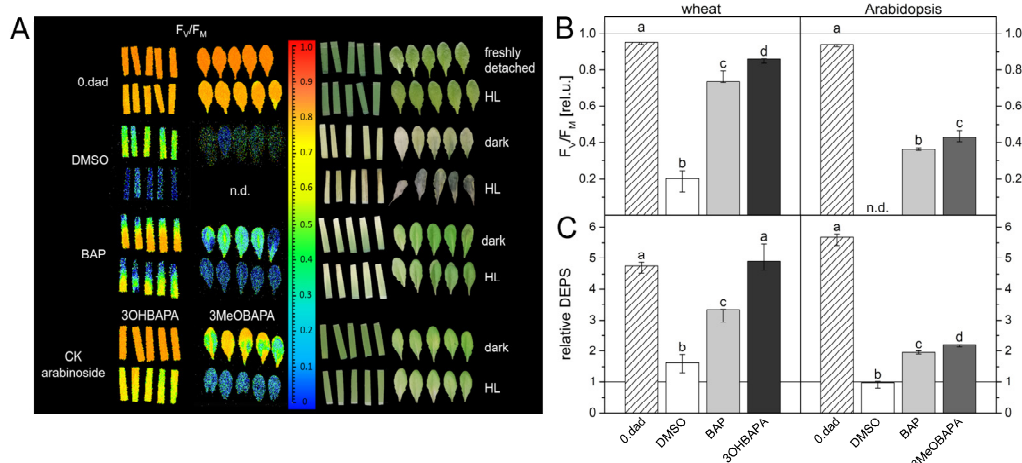


Figure 9. (A) Imaging of maximum quantum yield of PSII photochemistry (F_v/F_m) before and after high-light treatment (HL; 500 $\mu\text{mol photons}\cdot\text{m}^{-2}\cdot\text{s}^{-1}$ for 4 h) of freshly detached leaves and leaves incubated for 6 days in 0.1% DMSO or 10- $\mu\text{mol}\cdot\text{L}^{-1}$ solutions of BAP, 3OHBAPA or 3MeOBAPA; (B) the relative F_v/F_m values and (C) relative de-epoxidation state of xanthophylls (DEPS) in detached wheat and Arabidopsis leaves. The relative F_v/F_m and DEPS were calculated as a ratio of values measured after and before exposure to high light. In the column graphs, medians and quartiles estimated from presented values of individual leaves are shown ($n = 5$). Different letters indicate a statistically significant difference between treatments within a plant species ($p < 0.05$; Student's unpaired t -test).

In Arabidopsis, the xanthophyll cycle was only moderately stimulated in the 3MeOBAPA-treated leaves exposed to HL (Figure 9), so the protective effect of 3MeOBAPA seems to be associated with the lower excitation delivery to RCII (due to the decreased LHCII/RCII ratio) (Figure 4A) and to the maintenance of xanthophylls during HL treatment (Figure 10). On the other hand, the lower protection of the BAP-treated senescent leaves could be related to the increased excitation supply to RCII (Figure 4A) due to the maintained LHCII/RCII ratio. Under HL, photosynthetic apparatus in the BAP-treated senescent leaves was most probably overexcited, which could contribute to the lower protective effect of BAP against oxidative damage. This finding is consistent with our previous work, where we have shown that under excessive light conditions, the protective action of exogenous CKs on senescent leaves can switch to damaging [7,21] due to the overexcitation of photosynthetic apparatus and oxidative damage [7].

The effective anti-oxidative protection by BAPAs could be related to the upregulation of *JUB1*, *ELIP1* and *ELIP2* detected in the 3MeOBAPA-treated Arabidopsis leaves (Table S1). The ROS-responsive transcription factor *JUB1* is considered to be a central longevity regulator in Arabidopsis that acts through the modulation of H_2O_2 level in cells [40]. It has been found that the overexpression of *JUB1* not only delays senescence, but also enhances tolerance to abiotic stresses [40].

Early-light-induced proteins (ELIPs) belong to the family of pigment-protein LHCs and fulfill a protective function and prevent oxidative damage under conditions of excess light [41]. The photoprotective function of ELIPs is based on the transient binding of free Chl and was originally thought to be important predominantly for developing leaves (e.g., [42]). However, the protective role of ELIPs was also reported during senescence, although their upregulation was conditioned by the presence of light [43] and/or correlated with light intensity [44]. Surprisingly, 3MeOBAPA upregulated *ELIPs* even in the dark, indicating that some aspects of 3MeOBAPA actions are similar to the effect of increased light. Additionally, the reduction in the LHCII/RCII ratio, observed in 3MeOBAPA-treated leaves, is typical for leaf acclimation to high-light intensities. This 3MeOBAPA-induced response may help leaves to cope with subsequent (photo)oxidative stress. Additionally, 3MeOBAPA has been shown to protect human dermal fibroblasts from UV-A and UV-B treatment [25], thus the protective

activity of this compound may be more universal. The mechanism of this 3MeOBAPA effect remains to be elucidated.

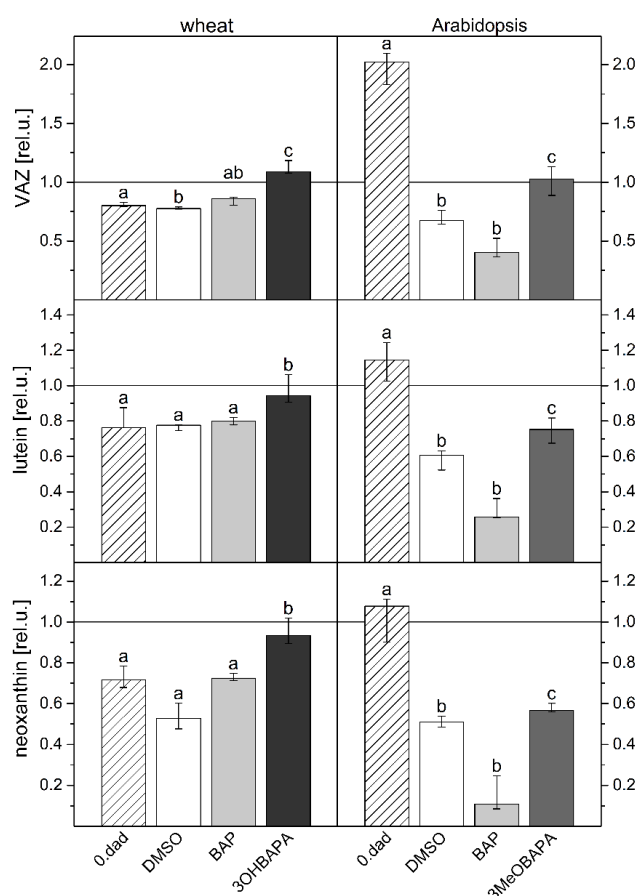


Figure 10. Violaxanthin, antheraxanthin, zeaxanthin (VAZ), lutein, and neoxanthin content (related to the value before high-light treatment) in control (0. dad) and detached leaves of wheat and Arabidopsis incubated in 0.1% DMSO or $10\text{-}\mu\text{mol}\cdot\text{L}^{-1}$ solutions of BAP, 3OHBAPA or 3MeOBAPA. Leaves were kept in the dark for 6 days and subsequently exposed to high light ($500\text{ }\mu\text{mol photons}\cdot\text{m}^{-2}\cdot\text{s}^{-1}$ for 4 h). Medians and quartiles are presented ($n = 4\text{--}5$). Different letters indicate a statistically significant difference between treatments within a plant species ($p < 0.05$; Student's unpaired t -test).

2.4. On the Mechanism of Specific Anti-Senescence Activity of CK Arabinosides

In our previous work, we have shown that the unique mode of CK arabinosides' action differs from that of CKs. The CK arabinosides were shown to have only low activity in the *Amaranthus* and callus CK bioassays [25,26]. However, their activity in the senescence bioassay was high, despite the fact that in vitro they did not activate the AHK3 receptor [26], which is considered to be the main receptor involved in CK-mediated delay of senescence [2,45] and protection during HL stress [46]. The RNA-seq gene expression analysis performed by Bryksová [26] in Arabidopsis 3MeOBAPA-treated leaves revealed a broad range of transcriptomic changes typical for the activation of the PAMP-response: downregulation of a number of photosynthetic genes and upregulation of many defense genes. A similar response can be expected in BAPAs-treated wheat and barley plants, as their enhanced resistance to pathogens was observed in field trial experiments [26].

The upregulation of genes of defense regulons in the 3MeOBAPA-treated Arabidopsis leaves included jasmonate/ethylene-driven upregulation of plant defensins and was accompanied by a significant elevation of endogenous levels of jasmonic acid (JA) and its metabolites [26]. However, as we have demonstrated here, the ethylene production in the BAPA-treated leaves was low, which might

be one of the main reasons for the BAPAs' high anti-senescence activity, as ethylene is known to promote leaf senescence [35]. It has been reported that the key transcription factor of the ethylene signaling pathway *EIN3* and its downstream target *ORE1* directly activate genes of Chl degradation. *ORE1* also directly promotes ethylene synthesis and ethylene in turn accelerates leaf senescence through *EIN3–ORE1* [47]. *EIN3* and *ORE1* were downregulated by 3MeOBAPA (Table S1), which indicates that the attenuation of this loop is involved in the anti-senescence activity of 3MeOBAPA. This activity is also evidenced by the downregulation of other positive regulators of senescence, such as *SAG12*, *ORE3*, and *ORE9* (Table S1). In summary, in this work we show for the first time that the anti-senescence effect of CK arabinosides in Arabidopsis may be related to specific downregulation of the *EIN3–ORE1* pathway which has been previously shown to be involved in leaf degreening through Chl catabolic gene regulation [47].

Similarly to ethylene, JA is considered to be a positive regulator of leaf senescence. As mentioned, the level of JA and its metabolites was found to be increased in the 3MeOBAPA-treated Arabidopsis leaves [26]. However, this increase was only temporary—it was observed after 48 h of the treatment [26], while after 4 days the JA level was lower than that in the mock-treated leaves (unpublished data). The transient increase in endogenous JA content appears to be involved in triggering the defense response by 3MeOBAPA and does not stimulate, but rather suppresses, leaf senescence. This hypothesis is in line with the upregulation of the JA-signalling repressors *JAZ7* and *JAZ 8* (Table S1), as *JAZ7* is known to be a specific negative regulator of dark-induced leaf senescence and together with *JAZ8* suppresses the activation of *SAGs* including *SAG12* [48,49].

The specific effects of CK arabinosides described in this work represent further evidence that they act through a mechanism different from that of classical CKs. Because they have high anti-senescence activity and protective effects under stress conditions and simultaneously do not impair root development, they are promising substances for plant protection. However, further study is needed to elucidate the exact mechanism of their action.

3. Materials and Methods

3.1. Plant Material

Plants of spring wheat (*Triticum aestivum* L. cv. Aranka) were grown on an artificial medium composed of perlite and Hoagland's solution in a growth chamber at 25 °C under a 16-h light (120 $\mu\text{mol photons}\cdot\text{m}^{-2}\cdot\text{s}^{-1}$)/8-h dark cycle for 7 days. Then segments were cut off from the primary leaves, 4 cm from the leaf tip. The basal end of the leaf segment was placed into a well of 96-well plate with 200 μL of 10- $\mu\text{mol}\cdot\text{L}^{-1}$ solutions of BAP, 3OHBAPA or 3MeOBAPA dissolved in 0.1% dimethylsulfoxide (DMSO; Sigma-Aldrich, St. Louis, MO, USA) or with 0.1% DMSO solution in deionized water (mock control). 3OHBAPA and 3MeOBAPA (Figure 1) were prepared as described previously [25,26]. The segments were kept in darkness at 24 °C for 6 days. Plants of *Arabidopsis thaliana* L. (Col-0) were grown in a soil (Potgrond H, Klasmann-Deilmann, Geeste, Germany) in a growth chamber under an 8-h light (120 $\mu\text{mol photons}\cdot\text{m}^{-2}\cdot\text{s}^{-1}$)/16-h dark cycle and at 22 °C/20 °C for 6 weeks. Then the 7th and 8th rosette leaves were detached from the plants and incubated in a six-well plate with 5 mL of the solutions described above. Freshly detached Arabidopsis and wheat leaves were used as control (0. day after detachment; dad).

3.2. High-Light Treatment

After six days in the dark, wheat leaf segments and Arabidopsis leaves incubated in the solutions described above were exposed to high-light (HL; white light, 500 $\mu\text{mol photons}\cdot\text{m}^{-2}\cdot\text{s}^{-1}$) for up to 8 h to induce photo-oxidative stress. In the case of wheat, edges of the segments were cut off and the rectangular middle part (2 cm long) of the leaf segment was placed into solutions prior to the HL treatment.

3.3. Determination of Chlorophyll, Carotenoid and Xanthophyll Content

Following estimation of their area, leaf samples were frozen in liquid nitrogen, stored at $-80\text{ }^{\circ}\text{C}$ and subsequently homogenized using 80% acetone and a small amount of MgCO_3 . Homogenate was centrifuged at $3600\times g$ for 15 min at $4\text{ }^{\circ}\text{C}$. The supernatant was used for spectrophotometric (Unicam UV 500, Thermo Spectronics, Cambridge, UK) estimation of Chl and carotenoid contents according to Lichtenthaler [50] and for quantification of xanthophylls (violaxanthin, V; antheraxanthin, A; zeaxanthin, Z; neoxanthin; lutein) by a reversed-phase high-performance liquid chromatography (HPLC) using Alliance e 2695 HPLC System (Waters, Milford, MA, USA) equipped with 2998 Photodiode Array detectors. The separation was carried out using a gradient system ($1.5\text{ mL}\cdot\text{min}^{-1}$ at $25\text{ }^{\circ}\text{C}$) on a LiChrospher[®] 100 RP-18 ($5\text{ }\mu\text{m}$) LiChroCART[®] 250-4 (Merck, Darmstadt, Germany). Quantification was performed by absorbance at the following wavelength: 437 (neoxanthin), 441 (violaxanthin), 446 (antheraxanthin), 447 (lutein), and 454 nm (zeaxanthin) using standards purchased from DHI Lab Products (Hørsholm, Denmark). The de-epoxidation state of xanthophylls (DEPS) was calculated as $\text{DEPS} = (\text{A} + \text{Z})/(\text{V} + \text{A} + \text{Z})$ [51].

3.4. Confocal Laser Scanning Microscopy

Confocal microscopy was performed on detached leaves kept in the dark for 6 days and on leaves subsequently exposed to HL for 4 h. Using fluorescent probe SPY-LHP (swallow-tailed perylene derivative; Dojindo Molecular Technologies, Rockville, MD, USA), lipid hydroperoxides (LOOHs) were localized. Wheat and Arabidopsis leaves were cut into pieces (approximately $2\text{ mm} \times 2\text{ mm}$) and incubated in $50\text{ }\mu\text{mol}\cdot\text{L}^{-1}$ SPY-LHP in HEPES buffer ($10\text{ m}\text{ }\mu\text{mol}\cdot\text{L}^{-1}$, pH 7.5) in the dark at room temperature for 30 min. Afterward, the samples were visualized by a confocal microscope (FV1000, Olympus Czech Group, Prague, Czech Republic). The excitation of fluorochrome was performed using a 488-nm line of argon laser. The signal was detected through a 505–550-nm emission filter. The morphology of tissues was visualized by a 405-nm diode laser excitation in transmitted light detection module with differential interference contrast (DIC) filters, while chloroplasts by a 543-nm helium–neon laser excitation with emission recorded with a 655–755-nm bandpass filter. The proper intensity of the laser was set according to unstained samples at the beginning of each experiment [52]. During the image postprocessing in FV10-ASW 4.0 Viewer software (Olympus Czech Group, Prague, Czech Republic), the contrast of the SPY-LHP channel was increased to 3 in the case of wheat and to 4 in the case of Arabidopsis. Five replicates were performed and representative images are presented.

3.5. Chlorophyll Fluorescence Parameters (PSII Functioning)

Chl fluorescence induction transient (OJIP curve) and Chl fluorescence quenching analysis were measured at room temperature from the adaxial side of the leaves using a Plant Efficiency Analyser (Hansatech Instruments, Norfolk, UK) and FluorCam imaging system (PSI, Drásov, Czech Republic), respectively. The control leaves and HL-treated leaves were dark-adapted for 30 min prior to the measurement. In the case of senescent leaves, dark adaptation was not necessary due to their incubation in the dark.

The OJIP transient was measured in the middle of leaf segments with excitation light (red light, $4300\text{ }\mu\text{mol photons}\cdot\text{m}^{-2}\cdot\text{s}^{-1}$) lasting 1 s. The initial slope of the O–J Chl fluorescence rise $(\text{dV}/\text{dt})_0$ and the relative variable fluorescence at the J step (V_J) were evaluated. The $(\text{dV}/\text{dt})_0$ parameter, defined as the maximal rate of accumulation of closed (i.e., reduced) RCII, was calculated as $(\text{dV}/\text{dt})_0 = 4 (F_{300\mu\text{s}} - F_{50\mu\text{s}})/F_V$, where $F_{300\mu\text{s}}$ and $F_{50\mu\text{s}}$ are fluorescence intensities at the indicated times of the transient, and F_V is variable fluorescence ($F_V = F_P - F_0$, where F_P is fluorescence intensity at P step and F_0 is minimal fluorescence) [28]. The V_J parameter reflects a fraction of reduced RCII and was calculated as $V_J = (F_J - F_0)/F_V$, where F_J is fluorescence intensity at 2 ms (J-step).

A FluorCam imaging system was used for the measurement of quantum yields Φ_P , Φ_{NPQ} and $\Phi_{f,D}$ reflecting the proportion of three different types of energy usage by PSII (their sum equals 1; [30]) in light-adapted state of senescent leaves, and for measurement of changes in maximum quantum yield of PSII photochemistry ($F_V/F_M = (F_M - F_0)/F_M$) after HL treatment (4 h). The effective quantum yield of PSII photochemistry for the light-adapted state was calculated as $\Phi_P = (F_M' - F_t)/F_M'$. The quantum yield of regulatory light-induced non-photochemical quenching was calculated as $\Phi_{NPQ} = (F_t/F_M') - (F_t/F_M)$. The quantum yield of constitutive non-regulatory dissipation processes was calculated as $\Phi_{f,D} = F_t/F_M$. The minimal fluorescence of the dark-adapted leaf sample (F_0) was determined by applying several μ -seconds-long measuring flashes (red light, $0.1 \mu\text{mol photons}\cdot\text{m}^{-2}\cdot\text{s}^{-1}$) at the beginning of the procedure. The maximal fluorescence of the dark-adapted sample (F_M) was measured using the 1.6-s saturating pulse (white light, $850 \mu\text{mol photons}\cdot\text{m}^{-2}\cdot\text{s}^{-1}$). After 2 min of dark relaxation the sample was exposed to actinic light (red light, $200 \mu\text{mol photons}\cdot\text{m}^{-2}\cdot\text{s}^{-1}$) and series of saturating pulses (the 1st pulse at the 3rd second of actinic light, 6 pulses in a 23-s interval, 3 pulses in a 47-s interval and the last 2 pulses in a 70-s interval) to measure the maximal fluorescence in the light-adapted sample (F_M'). The actual fluorescence signal at the time t of actinic illumination (F_t) was measured immediately prior to the application of saturating pulse. The last measured (steady-state) values of Φ_P , Φ_{NPQ} and $\Phi_{f,D}$ are presented.

3.6. Ethylene Production

The detached leaves of wheat and Arabidopsis were put into $10\text{-}\mu\text{mol}\cdot\text{L}^{-1}$ solutions of BAP, 3OHBAPA, 3MeOBAPA, or into 0.1% DMSO solution in distilled water and kept sealed in 8-mL vials in darkness for 6 days. Subsequently, 1.5 mL of air was collected from each vial and reduced to 1 mL before injection to gas-chromatograph Agilent GC 6890 (Agilent Technologies, Santa Clara, CA, USA) equipped with a flame ionization detector and 50-m capillary column (HP-AL/S stationary phase, $15 \mu\text{m}$, i.d. = 0.535). The injection temperature was set to $200 \text{ }^\circ\text{C}$, oven temperature to $40 \text{ }^\circ\text{C}$, and the detector temperature to $220 \text{ }^\circ\text{C}$. The measurements were performed in triplicate from three different test tubes of each variant.

3.7. Ultra-Weak Photon Emission

Two-dimensional imaging of ultra-weak photon emission (UPE) [53] was measured from the adaxial side of the leaves kept in the dark for 6 days before and after their treatment with $5\text{-mmol}\cdot\text{L}^{-1}$ H_2O_2 . After the first UPE measurement, the leaf segments were let to dry off for 30 min under common laboratory conditions and then put into the H_2O_2 solution. After 3 h of H_2O_2 incubation, the second UPE measurement was performed while the leaves remained in the H_2O_2 solution. A ratio of UPE of the leaf after and before the H_2O_2 incubation was estimated. The UPE was detected by a highly sensitive CCD camera VersArray 1300B (Princeton Instruments Trenton, NJ, USA) equipped with an objective (F mount Nikkor 50 mm, $f/1.2$, Nikon, Tokyo, Japan). The CCD element was cooled down to $-104 \text{ }^\circ\text{C}$ to reduce the background noise, the accumulation time of each measurement was 30 min. The UPE of the leaf represents the average number of counts from the leaf surface.

3.8. Ion Leakage

For the determination of the extent of ion leakage from leaf tissue as a measure of cell membrane damage, circular (diameter of 1 cm) or rectangular (2 cm long) segments were cut out from Arabidopsis leaves or wheat leaf segments, respectively. Groups of six leaf discs or eight rectangular segments (one group represents one sample) were put into 6-well plates containing 3.5 mL of deionized water and incubated under HL ($500 \mu\text{mol photons}\cdot\text{m}^{-2}\cdot\text{s}^{-1}$) for up to 8 h to induce oxidative damage in cell membranes. The conductivity of the solutions was measured after 2, 4, 6 and 8 h of the HL treatment with a conductivity meter (GMH 3430, Greisinger, Regenstauf, Germany). As DMSO is known to affect the membrane fluidity and permeability for ions, deionized water was used as a mock control as well to exclude effect of DMSO on the membrane permeability.

Supplementary Materials: Supplementary materials can be found at <http://www.mdpi.com/1422-0067/21/21/8109/s1>.

Author Contributions: Z.K. and M.Š. designed the experiments, analyzed and interpreted the data and wrote the article. Z.K. prepared samples for all experiments, performed Chl fluorescence and ion leakage measurements. M.R. performed UPE analysis and confocal microscopy. J.M. performed analysis of ethylene production. P.P. performed pigment analysis by HPLC. M.B. synthesized the CK arabinosides. M.S. supervised the confocal microscopy measurement. K.D. supervised the CK arabinoside synthesis and experimental design. O.P. contributed to the critical revision of the manuscript. All authors have read and agreed to the published version of the manuscript.

Funding: The work was funded by ERDF projects “Plants as a tool for sustainable global development” (No. CZ.02.1.01/0.0/0.0/16_019/0000827) and “Development of pre-applied research in nanotechnology and biotechnology” (No. CZ.02.1.01/0.0/0.0/17_048/0007323); Czech Science Foundation grant 16-04184S (O.P. and K.D.); IGA_PrF_2018_022 (Z.K. and Ma.Š.) and IGA_PrF_2020_010 (M.B. and K.D.).

Acknowledgments: We would like to thank Pavla Ocvirková for her skillful technical assistance.

Conflicts of Interest: The authors declare no conflict of interest. The funders had no role in the design of the study; in the collection, analyses, or interpretation of data; in the writing of the manuscript, or in the decision to publish the results.

Abbreviations

A	antheraxanthin
AHK	Arabidopsis histidine kinase
BAP	6-benzylaminopurine
car	carotenoid
Chl	chlorophyll
CK	cytokinin
dad	day after detachment
DEPS	de-epoxidation state of xanthophylls
DIC	differential interference contrast
DMSO	dimethylsulfoxide
$(dV/dt)_0$	the initial slope of the O–J Chl fluorescence rise
F_V/F_M	the maximum quantum yield of photosystem II photochemistry
HL	high light
JA	jasmonic acid
LHCII	light-harvesting complexes of photosystem II
LOOH	lipid hydroperoxide
OJIP	chlorophyll fluorescence induction transient
PSII	photosystem II
Q_A	primary electron acceptor of photosystem II
RCII	reaction center of photosystem II
SAG	senescence-associated gene
UPE	ultra-weak photon emission
V	violaxanthin
V_J	the relative variable fluorescence at the J step of OJIP curve
Z	zeaxanthin
3OHBAPA	6-(3-hydroxybenzylamino)-9- β -D-arabinofuranosylpurine
3MeOBAPA	6-(3-methoxybenzylamino)-9- β -D-arabinofuranosylpurine
$\Phi_{f,D}$	the quantum yield of constitutive non-regulatory dissipation processes
Φ_{NPQ}	the quantum yield of regulatory light-induced non-photochemical quenching
Φ_P	the effective quantum yield of photosystem II photochemistry (for the light-adapted state)

References

1. Špundová, M.; Popelková, H.; Ilík, P.; Skotnica, J.; Novotný, R.; Nauš, J. Ultra-structural and functional changes in the chloroplasts of detached barley leaves senescing under dark and light conditions. *J. Plant Physiol.* **2003**, *160*, 1051–1058. [[CrossRef](#)] [[PubMed](#)]
2. Janečková, H.; Husičková, A.; Ferretti, U.; Prčina, M.; Pilařová, E.; Plačková, L.; Pospíšil, P.; Doležal, K.; Špundová, M. The interplay between cytokinins and light during senescence in detached *Arabidopsis* leaves. *Plant Cell Environ.* **2018**, *41*, 1870–1885. [[CrossRef](#)] [[PubMed](#)]
3. Janečková, H.; Husičková, A.; Lazar, D.; Ferretti, U.; Pospíšil, P.; Špundová, M. Exogenous application of cytokinin during dark senescence eliminates the acceleration of photosystem II impairment caused by chlorophyll b deficiency in barley. *Plant Physiol. Biochem.* **2019**, *136*, 43–51. [[CrossRef](#)] [[PubMed](#)]
4. Breeze, E.; Harrison, E.; McHattie, S.; Hughes, L.; Hickman, R.; Hill, C.; Kiddle, S.; Kim, Y.S.; Penfold, C.A.; Jenkins, D.; et al. High-resolution temporal profiling of transcripts during *Arabidopsis* leaf senescence reveals a distinct chronology of processes and regulation. *Plant Cell* **2011**, *23*, 873–894. [[CrossRef](#)] [[PubMed](#)]
5. Holub, L.; Hanuš, J.; Hanke, D.E.; Strnad, M. Biological activity of cytokinins derived from *ortho*- and *meta*-hydroxybenzyladenine. *Plant Growth Regul.* **1998**, *26*, 109–115. [[CrossRef](#)]
6. Oh, M.H.; Kim, J.H.; Zulfugarov, I.S.; Moon, Y.H.; Rhew, T.H.; Lee, C.H. Effects of benzyladenine and abscisic acid on the disassembly process of photosystems in an *Arabidopsis* delayed-senescence mutant, *ore9*. *J. Plant Biol.* **2005**, *48*, 170–177. [[CrossRef](#)]
7. Vlčková, A.; Špundová, M.; Kotabová, E.; Novotný, R.; Doležal, K.; Nauš, J. Protective cytokinin action switches to damaging during senescence of detached wheat leaves in continuous light. *Physiol. Plant.* **2006**, *126*, 257–267. [[CrossRef](#)]
8. Zavaleta-Mancera, H.A.; López-Delgado, H.; Loza-Tavera, H.; Mora-Herrera, M.; Trevilla-García, C.; Vargas-Suárez, M.; Ougham, H. Cytokinin promotes catalase and ascorbate peroxidase activities and preserves the chloroplast integrity during dark-senescence. *J. Plant Physiol.* **2007**, *164*, 1572–1582. [[CrossRef](#)] [[PubMed](#)]
9. Liu, L.; Li, H.; Zeng, H.; Cai, Q.; Zhou, X.; Yin, C. Exogenous jasmonic acid and cytokinin antagonistically regulate rice flag leaf senescence by mediating chlorophyll degradation, membrane deterioration, and senescence-associated genes expression. *J. Plant Growth Regul.* **2016**, *35*, 366–376. [[CrossRef](#)]
10. Weaver, L.M.; Gan, S.; Quirino, B.; Amasino, R.M. A comparison of the expression patterns of several senescence-associated genes in response to stress and hormone treatment. *Plant Mol. Biol.* **1998**, *37*, 455–469. [[CrossRef](#)]
11. Vylčilová, H.; Husičková, A.; Spíchal, L.; Srovnal, J.; Doležal, K.; Plíhal, O.; Plíhalová, L. C2-substituted aromatic cytokinin sugar conjugates delay the onset of senescence by maintaining the activity of the photosynthetic apparatus. *Phytochemistry* **2016**, *122*, 22–33. [[CrossRef](#)]
12. Schippers, J.H.M.; Schmidt, R.; Wagstaff, C.; Jing, H.C. Living to die and dying to live: The survival strategy behind leaf senescence. *Plant Physiol.* **2015**, *169*, 914–930. [[CrossRef](#)]
13. Koprna, R.; De Diego, N.; Dundálková, L.; Spíchal, L. Use of cytokinins as agrochemicals. *Bioorg. Med. Chem.* **2016**, *24*, 484–492. [[CrossRef](#)]
14. Galuszka, P.; Popelková, H.; Werner, T.; Frébortová, J.; Pospíšilová, H.; Mik, V.; Köllmer, I.; Schmülling, T.; Frébort, I. Biochemical characterization of cytokinin oxidases/dehydrogenases from *Arabidopsis thaliana* expressed in *Nicotiana tabacum* L. *J. Plant Growth Regul.* **2007**, *26*, 255–267. [[CrossRef](#)]
15. Aremu, A.O.; Bairu, M.W.; Doležal, K.; Finnie, J.F.; Van Staden, J. Topolins: A panacea to plant tissue culture challenges? *Plant Cell Tissue Organ Cult.* **2012**, *108*, 1–16. [[CrossRef](#)]
16. Woodward, E.J.; Marshall, C. Effects of plant-growth regulators and nutrient supply on tiller bud outgrowth in barley (*Hordeum distichum* L.). *Ann. Bot.* **1998**, *61*, 347–354. [[CrossRef](#)]
17. Werbrouck, S.P.O.; Strnad, M.; Van Ockelen, H.A.; Debergh, P.C. Meta-topolin, an alternative to benzyladenine in tissue culture? *Physiol. Plant.* **1996**, *98*, 291–297. [[CrossRef](#)]
18. Iqbal, M.; Ashraf, M.; Jamil, A. Seed enhancement with cytokinins: Changes in growth and grain yield in salt stressed wheat plants. *Plant Growth Regul.* **2006**, *50*, 29–39. [[CrossRef](#)]
19. Bairu, M.W.; Stirk, W.A.; Doležal, K.; Van Staden, J. Optimizing the micropropagation protocol for the endangered *Aloe polyphylla*: Can meta-topolin and its derivatives serve as replacement for benzyladenine and zeatin? *Plant Cell Tissue Organ. Cult.* **2007**, *90*, 15–23. [[CrossRef](#)]

20. Rulcová, J.; Pospíšilová, J. Effect of benzylaminopurine on rehydration of bean plants after water stress. *Biol. Plant.* **2001**, *44*, 75–81. [[CrossRef](#)]
21. Prokopová, J.; Špundová, M.; Sedlářová, M.; Husičková, A.; Novotný, R.; Doležal, K.; Nauš, J.; Lebeda, A. Photosynthetic responses of lettuce to downy mildew infection and cytokinin treatment. *Plant Physiol. Biochem.* **2010**, *48*, 716–723. [[CrossRef](#)] [[PubMed](#)]
22. Plíhalová, L.; Vylíčilová, H.; Doležal, K.; Zahajská, L.; Zatloukal, M.; Strnad, M. Synthesis of aromatic cytokinins for plant biotechnology. *N. Biotechnol.* **2016**, *33*, 614–624. [[CrossRef](#)] [[PubMed](#)]
23. Tarkowská, D.; Doležal, K.; Tarkowski, P.; Āstot, C.; Holub, J.; Fuksová, K.; Schmölling, T.; Sandberg, G.; Strnad, M. Identification of new aromatic cytokinins in *Arabidopsis thaliana* and *Populus x canadensis* leaves by LC-(+)-ESI-MS and capillary liquid chromatography frit-fast atom bombardment mass spectrometry. *Physiol. Plant.* **2003**, *117*, 579–590. [[CrossRef](#)] [[PubMed](#)]
24. Szüčová, L.; Spíchal, L.; Doležal, K.; Zatloukal, M.; Greplová, J.; Galuszka, P.; Kryštof, V.; Voller, J.; Popa, I.; Massino, F.J.; et al. Synthesis, characterization and biological activity of ring-substituted 6-benzylamino-9-tetrahydropyran-2-yl and 9-tetrahydrofuran-2-ylpurine derivatives. *Bioorg. Med. Chem.* **2009**, *17*, 1938–1947. [[CrossRef](#)]
25. Doležal, K.; Plíhalová, L.; Vylíčilová, H.; Zatloukal, M.; Plíhal, O.; Voller, J.; Strnad, M.; Bryksová, M.; Vostálová, J.; Rajnochová Svobodová, A.; et al. 6-aryl-9-glycosylpurines and use thereof. U.S. Patent 10,100,077, 16 October 2018.
26. Bryksová, M.; Dabravolski, S.; Kučerová, Z.; Zavdil Kokáš, F.; Špundová, M.; Plíhalová, L.; Takáč, T.; Grúz, J.; Hudeček, M.; Hloušková, V.; et al. Aromatic cytokinin arabinosides promote PAMP-like responses and positively regulate leaf longevity. *ACS Chem. Biol.* **2020**, *15*, 1949–1963. [[CrossRef](#)]
27. Nisler, J.; Zatloukal, M.; Sobotka, R.; Pilný, J.; Zdvihalová, B.; Novák, O.; Strnad, M.; Spíchal, L. New urea derivatives are effective anti-senescence compounds acting most likely via a cytokinin-independent mechanism. *Front. Plant Sci.* **2018**, *9*, 1225. [[CrossRef](#)]
28. Strasser, R.J.; Srivastava, A.; Tsimilli-Michael, M. The fluorescence transient as a tool to characterize and screen photosynthetic samples. In *Probing Photosynthesis: Mechanism, Regulation & Adaptation*; Yunus, M., Pathre, U., Mohanty, P., Eds.; Taylor & Francis: New York, NY, USA, 2000; pp. 443–480.
29. Leong, T.-Y.; Anderson, J.M. Adaptation of the thylakoid membranes of pea chloroplasts to light intensities. II. Regulation of electron transport capacities, electron carriers, coupling factor (CF1) activity and rates of photosynthesis. *Photosynth. Res.* **1984**, *5*, 117–128. [[CrossRef](#)]
30. Lazár, D. Parameters of photosynthetic energy partitioning. *J. Plant Physiol.* **2015**, *175*, 131–147. [[CrossRef](#)]
31. Triantaphylidès, C.; Havaux, M. Singlet oxygen in plants: Production, detoxification and signalling. *Trends Plant Sci.* **2009**, *14*, 219–228. [[CrossRef](#)]
32. Špundová, M.; Vlčková, A.; Doležal, K.; Habertová, A.; Nauš, J.; Strnad, M. Effect of meta-topolin and bohemine derived from benzylaminopurine on PSII function in artificially senescing wheat leaves. In *Proceedings of the 12th International Congress on Photosynthesis*; CSIRO Publishing: Collingwood, Victoria, Australia, 2001; S22-012.
33. Cary, J.A.; Liu, W.; Howell, S.H. Cytokinin action is coupled to ethylene in its effects on the inhibition of root and hypocotyl elongation in *Arabidopsis thaliana* seedlings. *Plant Physiol.* **1995**, *107*, 1075–1082. [[CrossRef](#)]
34. Zdarska, M.; Dobisová, T.; Gelová, Z.; Pernisová, M.; Dabravolski, S.; Hejátko, J. Illuminating light, cytokinin, and ethylene signalling crosstalk. *J. Exp. Bot.* **2015**, *66*, 4913–4931. [[CrossRef](#)] [[PubMed](#)]
35. Ceusters, J.; Van de Poel, B. Ethylene exerts species-specific and age-dependent control of photosynthesis. *Plant Physiol.* **2018**, *176*, 2601–2612. [[CrossRef](#)] [[PubMed](#)]
36. Wi, S.J.; Jang, S.J.; Park, K.Y. Inhibition of biphasic ethylene production enhances tolerance to abiotic stress by reducing the accumulation of reactive oxygen species in *Nicotiana tabacum*. *Mol. Cells* **2010**, *30*, 37–49. [[CrossRef](#)] [[PubMed](#)]
37. Pospíšil, P.; Prasad, A.; Rác, M. Role of reactive oxygen species in ultra-weak photon emission in biological systems. *J. Photoch Photobiol. B* **2014**, *139*, 11–23. [[CrossRef](#)] [[PubMed](#)]
38. Li, Z.; Wakao, S.; Fischer, B.B.; Niyogi, K.K. Sensing and responding to excess light. *Annu Rev. Plant Biol.* **2009**, *60*, 239–260. [[CrossRef](#)] [[PubMed](#)]
39. Pinnola, A.; Bassi, R. Molecular mechanisms involved in plant photoprotection. *Biochem. Soc. Trans.* **2018**, *46*, 467–482. [[CrossRef](#)]

40. Wu, A.; Allu, A.D.; Garapati, P.; Siddiqui, H.; Dortay, H.; Zanol, M.I.; Asensi-Fabado, M.A.; Munné-Bosch, S.; Antonio, C.; Tohge, T.; et al. JUNGBRUNNEN1, a reactive oxygen species-responsive NAC transcription factor, regulates longevity in Arabidopsis. *Plant Cell* **2012**, *24*, 482–506. [[CrossRef](#)]
41. Hutin, C.; Nussaume, L.; Moise, N.; Moya, I.; Kloppstech, K.; Havaux, M. Early light-induced proteins protect Arabidopsis from photooxidative stress. *Proc. Natl. Acad. Sci. USA* **2003**, *100*, 4921–4926. [[CrossRef](#)]
42. Meyer, G.; Kloppstech, K. A rapidly light-induced chloroplast protein with a high turnover coded for by pea nuclear DNA. *Eur. J. Biochem.* **1984**, *138*, 201–207. [[CrossRef](#)]
43. Binyamin, L.; Falah, M.; Portnoy, V.; Soudry, E.; Gepstein, S. The early light-induced protein is also produced during leaf senescence of *Nicotiana tabacum*. *Planta* **2001**, *212*, 591–597. [[CrossRef](#)]
44. Humbeck, K.; Kloppstech, K.; Krupinska, K. Expression of early-light inducible proteins in flag leaves of field-grown barley. *Plant Physiol.* **1994**, *105*, 1217–1222. [[CrossRef](#)]
45. Riefler, M.; Novák, O.; Strnad, M.; Schmölling, T. Arabidopsis cytokinin receptor mutants reveal functions in shoot growth leaf senescence, seed size, germination, root development, and cytokinin metabolism. *Plant Cell* **2016**, *18*, 40–54. [[CrossRef](#)] [[PubMed](#)]
46. Cortleven, A.; Nitschke, S.; Klaumünzer, M.; Abdelgawad, H.; Asard, H.; Grimm, B.; Riefler, M.; Schmölling, T. A novel protective function for cytokinin in the light stress response is mediated by the Arabidopsis histidine kinase2 and Arabidopsis histidine kinase3 receptors. *Plant Physiol.* **2014**, *164*, 1470–1483. [[CrossRef](#)] [[PubMed](#)]
47. Qiu, K.; Li, Z.; Yang, Z.; Chen, J.; Wu, S.; Zhu, X.; Gao, S.; Gao, J.; Ren, G.; Kuai, B.; et al. EIN3 and ORE1 accelerate degreening during ethylene-mediated leaf senescence by directly activating chlorophyll catabolic genes in Arabidopsis. *PLoS Genet.* **2015**, *11*, e1005399. [[CrossRef](#)]
48. Yu, J.; Zhang, Y.; Di, C.; Zhang, Q.; Zhang, K.; Wang, C.; You, Q.; Yan, H.; Dai, S.Y.; Yuan, J.S.; et al. JAZ7 negatively regulates dark-induced senescence in Arabidopsis. *J. Exp. Bot.* **2016**, *67*, 751–762. [[CrossRef](#)] [[PubMed](#)]
49. Kim, J.; Kim, J.H.; Lyu, J.I.; Woo, H.R.; Lim, P.O. New insights into the regulation of leaf senescence in Arabidopsis. *J. Exp. Bot.* **2018**, *69*, 787–799. [[CrossRef](#)] [[PubMed](#)]
50. Lichtenthaler, H.K. Chlorophylls and carotenoids: Pigments of photosynthetic biomembranes. *Methods Enzymol.* **1987**, *148*, 350–382. [[CrossRef](#)]
51. Gilmore, A.M.; Björkman, O. Adenine nucleotides and the xanthophyll cycle in leaves—I. Effects of CO₂- and temperature-limited photosynthesis on adenylate energy charge and violaxanthin de-epoxidation. *Planta* **1994**, *192*, 526–536. [[CrossRef](#)]
52. Sedlářová, M.; Petřivalský, M.; Piterková, J.; Luhová, L.; Kočířová, J.; Lebeda, A. Influence of nitric oxide and reactive oxygen species on development of lettuce downy mildew in *Lactuca* spp. *Eur. J. Plant Pathol.* **2011**, *129*, 267–280. [[CrossRef](#)]
53. Prasad, A.; Pospíšil, P. Towards the two-dimensional imaging of spontaneous ultra-weak photon emission from microbial, plant and animal cells. *Sci. Rep.* **2013**, *3*, 1211. [[CrossRef](#)]

Publisher’s Note: MDPI stays neutral with regard to jurisdictional claims in published maps and institutional affiliations.



© 2020 by the authors. Licensee MDPI, Basel, Switzerland. This article is an open access article distributed under the terms and conditions of the Creative Commons Attribution (CC BY) license (<http://creativecommons.org/licenses/by/4.0/>).